

CADMIUM CHALCOGENIDE THIN FILMS FOR POTENTIOMETRIC APPLICATIONS

M. ESSI^{a,*}, G. CISSE^{a,b}, V. FLAUD^c

^a*UFR-SSMT, Université Félix HOUPHOUET-BOIGNY de Cocody, 22 BP 582
Abidjan 22, Côte d'Ivoire*

^b*INRA, UMR Eco & Sols, INRA-IRD-Cirad-SupAgro, 2 Place Viala 34060
Montpellier. France*

^c*ICGM, Université Montpellier. 34000 Montpellier, France*

Sputtered nano devices based on chalcogenide glasses have been studied. Physical, chemical and electrochemical characteristics are presented. Cd-Ag-(Ge₂₈Sb₁₂Se₆₀) and Cd-Ag-(As₂S₃) miniaturised ion selective electrodes exhibit near-Nernstian response with a low detection limit versus cadmium (+II) species in solution. High reproducibility and high selectivity are observed. This is a favourable feature for measurements in natural water and waste effluents. Moreover, non-destructive in situ electrochemical technique that is capable of characterizing interfacial reactions has been successfully used. Indeed, Electrochemical Impedance Spectroscopy technique was used to provide information on fundamental processes that occur at the electrode – solution interface.

(Received June 14, 2020; Accepted October 5, 2020)

Keywords: Chalcogenide glass, Cd-SE, Micro sensor, Electrode – solution interface, Cadmium (+II) ion, Electrochemical impedance spectroscopy (EIS), Thin film

1. Introduction

Heavy metals are non-biodegradable, ubiquitously distributed and lead to a greater risk to human health and environment [1]. They get accumulated in the biosphere and enter living organisms through the alimentary chain. Several international organizations have included heavy metals as the priority substances to be monitored and have set certain permissible limits for their concentrations in agreement with the environmental quality standards [2]. In order to detect these toxic metal species many analytical techniques are being used [1]. But these techniques are expensive and time consuming. Electrochemical sensors can be employed to overcome the limitations of other methods. Potentiometric sensors are widely used in many areas, such as environmental monitoring, industrial factories, and wearable sensors [3]. They are easy to use and their interpretation of the out-put signals is straightforward. Potentiometric electrodes based on ion-selective electrodes have certain advantages like reproducibility and simple measuring technique [4]. Moreover, recent improvements in the detection limits of selective electrodes (ISEs) yield potentiometric sensors for direct determination of ions down to the low level [5, 6]. Chalcogenide glasses in combination with a suitable element are an important class of amorphous materials appropriate for many applications [7]. One approach to realize sensing membranes with high chemical stability offer ion-selective electrodes (ISE) based on chalcogenide materials. Consequently, ISEs with chalcogenide glasses are widely used for determination of heavy metal ions concentration in solutions [2, 8-10]. On the other hand, the combination of the sensors and circuits (called integrated micro sensors) represents an attractive approach in being able to realize compact sensitive devices. A variety of chalcogenide materials have been used as thin film micro sensors [11]. Then, the traditional ISEs could be miniaturised to a few microns by use of thin films techniques (i. e. RF sputtering, PLD) [2, 8, 12, 13]. There are net benefits to using glassy materials for micro ISE fabrication. From an electrical point of view the low impedance of a thin film compared to that of the corresponding bulk material allows the use of poor conducting glasses [14, 15]. In addition, electrical properties can be adjusted by doping control. The principal sensor aim

* Corresponding author: marc.essi@netcourrier.com

of present work is to develop reliable micro ISE for the determination of Cd^{2+} species in solution. Micro device is based on chalcogenide glass. RF sputtering allow the deposition of sensing thin membrane. The present paper deals with some original results in the laboratory and environmental applications of Cd-sensors. The use of electrochemical impedance spectroscopy (EIS) is highly desirable because it is a non-destructive in situ electrochemical technique that is able to characterize interfacial reactions and provides a corollary for the surface analysis results.

2. Experimental

Table 1. Process parameters for the thin films deposition.

Process parameters	Values
Deposition Pressure	5.10^{-2} mbar
Deposition Time	60 min
RF Power	25 W
Distance from the substrate to the target	5 cm
Argon flow rate	23 cm^3

RF sputtering is a physical vapor deposition process in which particles are ejected from a solid target material due to bombardment of energetic particles. Physical sputtering is driven by momentum exchange between the ions and atoms in the target material, due to collisions [16]. Voltage ionizes argon atoms and creates plasma. Then argon ions are accelerated towards chalcogenide target. The strong magnetic field confines dense plasma near the target. It tends to generate stable plasma with high density of argon ions and increases the efficiency of sputtering process. The substrates were cleaned using a standard cleaning procedure. Glass substrates were cleaned in ultra-sonic bath, degreased by detergent, deionised water and methanol-acetone-methanol for 5 minutes, respectively. Then, the cleaned glasses were dried. Substrates were immediately loaded into deposition chamber after cleaning. An Alcatel Dion 300 device equipped with a PFG 300 RF Huttinger, 13.56 MHz, 300 W generator was used. Cd-Ag- $[\text{Ge}_{28}\text{Sb}_{12}\text{Se}_{60}]$ and Cd-Ag- $[\text{As}_2\text{S}_3]$ sensing thin films were deposited by RF magnetron co-sputtering of the host glasses (i. e. $\text{Ge}_{28}\text{Sb}_{12}\text{Se}_{60}$, As_2S_3) and metallic alloys (i. e. cadmium, silver). The degree of vacuum is 10^{-6} mbar. During the process, the sputtering power is 25W and the chamber pressure was fixed to be 5.10^{-2} mbar (Table 1). A low sputtering power is observed considering the insulator character of chalcogenide materials. Target was kept facing substrate holder 5 cm away. Pre-sputtering for 10 minutes was carried out in order to remove the target surface contamination before the main deposition.

Response characteristics of micro sensor have been measured using standard ion-selective potentiometry using thin-film micro electrode in conjunction with a reference electrode [17]. All measurements were performed with a conventional double-liquid junction Ag/AgCl reference electrode. The out-put signal of the measurement chain was recorded with a highly ohmic multimeter versus different Cd^{2+} ions concentrations in the range from 10^{-7} to 10^{-3} M. As a background electrolyte, KNO_3 10^{-1} M was used together with the respective $\text{Cd}(\text{NO}_3)_2$ concentration. All chemicals used were of a reagent grade. The measured ISE potential is the sum of the reference electrode potentials, the membrane potential constituted by boundary potentials at each membrane - solution interface, and a possible diffusion potential which may be caused by an ion concentration gradient with in the sensing material phase.

Electrochemical impedance spectroscopy is a non-destructive steady-state technique that is able to provide in situ data on relaxation phenomena over a large range of frequencies [4]. EIS studies were undertaken using Potentiostat/Galvanostat apparatus (PGSTAT100, Autolab) coupled with a response analyser in frequency. A metallic wire was used as the auxiliary electrode with the

micro sensor and the double-liquid junction Ag/AgCl reference electrode. Room temperature EIS data were collected at the open circuit potential.

3. Results

The thickness of deposited thin films was found to be 350 nm which was confirmed from SEM cross sectional images. The thickness increases monotonically with increase in deposition time and depends on the operating pressure during sputtering besides RF power. These results have been reported for RF magnetron chalcogenide sputtered films. [18].

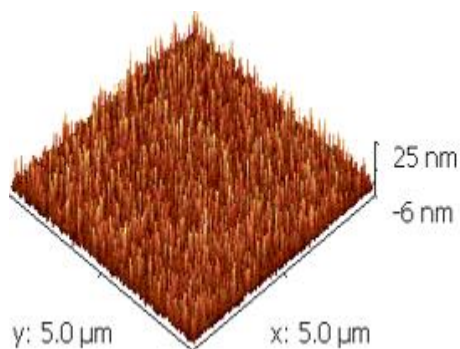


Fig. 1. 3D AFM image of Cd-Ag($Ge_{28}Sb_{12}Se_{60}$) thin film.

The morphology and topography of the sensing chalcogenide membranes were examined. As shown in figure 1 the rms roughness of the layers determined by atomic force microscopy (AFM) was on the order of 2-3 nm order. It was found that the surface roughness increases with deposition time showing the enhancement in the texture of the micro films. During the sputter deposition the roughening of the film growth is due to interplay of the uncorrelated growth of the particles, smoothing by the surface diffusion and also due to the shadowing effects. The surface morphology of the as-prepared membranes was examined under scanning electron microscopy (SEM). All SEM images [i. e. figure. 2 (a, b, c and d)] show the formation of smooth, continuous and dense films without cracks. To confirm the formation of nanometer size particles, transmission electron microscopy (TEM) analysis was performed. The study exhibits randomly distributed spherical nanoparticles in agreement with the columnar structure. Moreover the surface morphology exhibits pinholes, and grain boundaries.

X-ray diffraction (XRD) patterns were analysed in order to determine the structural and crystallographic properties. According to XRD spectra as no significant peaks were observed for the as-deposited films depicting an amorphous nature. The amorphous films revealed homogeneous chemical composition. The films exhibited non-induced optical anisotropy, which can arise from birefringence [19, 20]. The composition of the deposited films corresponded reasonably well with the expected stoichiometry.

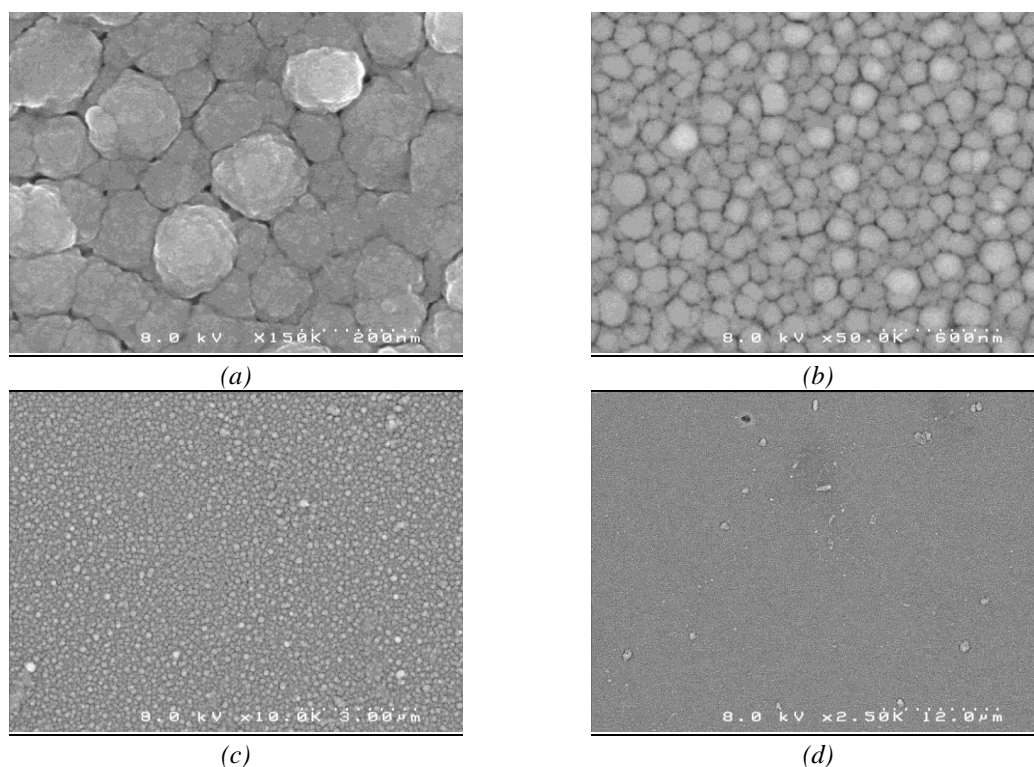


Fig. 2. 2D SEM images of Cd-Ag.(Ge₂₈Sb₁₂Se₆₀) thin film.

The use of a silver electrode as thin film collector seems the most suitable to provide an unhindered transition from ionic conductivity of the sensitive membrane to electronic conductivity of the metal contact. It is clearly evident that the interface plays the part of a pseudo-internal reference electrode. The electrochemical characterization of the micro electrodes was done by means of potentiometry. Therefore, the potential was recorded depending on the time and the varying Cd (+II) ion concentration. Figs. 3(a) and 3(b) show Cd²⁺ ion response for Cd-chalcogenide sensors. Both Cd-As₂S₃ and Cd-Ge₂₈Sb₁₂Se₆₀ thin membranes exhibit worst behaviour with weak sensitivity. However the shapes of the curves are satisfying. Worst signal might be due to micro sensor low conductivity in comparison to Cu-Ge₂₈Sb₁₂Se₆₀ and Cu-As₂S₃ systems [21-23]. To enhance sensor conductivity silver was added to film composition.

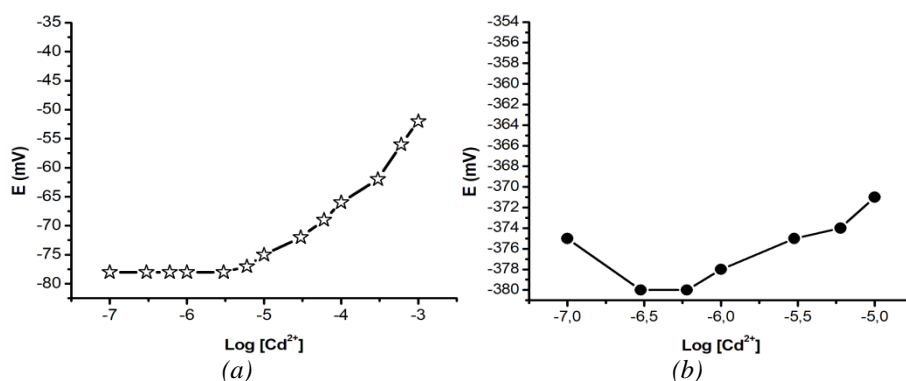


Fig. 3. Calibration curves of micro sensors (Cd-As₂S₃ (a) and Cd-Ge₂₈Sb₁₂Se₆₀ (b)).

Figs. 4(a) and 4(b) present out-put signal of fresh-deposited nano materials. Both as-prepared sensing thin devices (i. e. Cd-Ag-As₂S₃ and Cd-Ag-Ge₂₈Sb₁₂Se₆₀) immediately exhibit

primary ion response. However, the first calibrations of the unconditioned micro sensors differ from the further ones by the super Nernstian response at low Cd^{2+} concentration. After subsequent measurements the ISE parameters are constant and reliable in agreement with Nernst theory. Indeed, as shown in figures 4(c), 4(d) and table 2, in static measurements near Nernstian response is observed with a great limit of detection. Then, electrodes displayed stable and reproducible response. The sensing mechanism of chalcogenide glass-based potentiometric ISEs can be explained by the so-called modified surface layer model. The modified surface layer (MSL) appears on the membrane surface after the contact with the analysed electrolyte. During MSL formation a super Nernstian sensor response is observed. Moreover, MSL results from the interaction taking place between the solution of the potential-determining ion and the partially destroyed glassy network, which is accompanied by the creation of active exchange centers. The ionic sensitivity is defined by the direct exchange of the respective potential-determining ion between the test analyte and the membrane surface. [3, 14]. Indeed, Nernstian out-put signal is observed when MSL formation is completed.

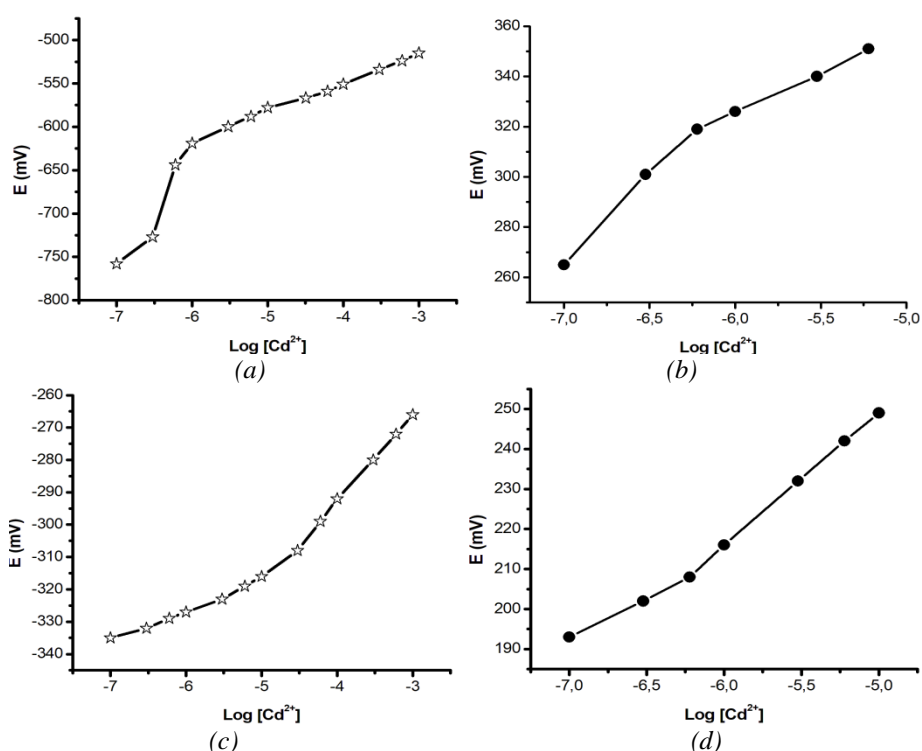


Fig. 4. Calibration curves of micro sensors $\text{Cd-Ag-As}_2\text{S}_3$ [as-prepared thin film (a) and optimum out-put signal (c)] and $\text{Cd-Ag-Ge}_{28}\text{Sb}_{12}\text{Se}_{60}$ [as-prepared thin film (b) and optimum out-put signal (d)].

Table 2. Micro sensor performance of $\text{Cd-Ag-As}_2\text{S}_3$ and $\text{Cd-Ag-Ge}_{28}\text{Sb}_{12}\text{Se}_{60}$.

	$\text{Cd-Ag-As}_2\text{S}_3$	$\text{Cd-Ag-Ge}_{28}\text{Sb}_{12}\text{Se}_{60}$
Sensitivity (mV/dec)	29	27
Response time (s)	10	10
Drift (mV/48H)	15	13
Detection Limit (mol/L)	10^{-6}	3.10^{-7}

In order to investigate the performance of the microelectrode characteristics, various operation parameters were tested. As expected all the thin film devices exhibit high selectivity in the presence of alkali, alkaline-earth, Ti^+ , Fe^{3+} ions and are less influenced by strong oxidizers. Copper (+II) ions influence the Cadmium (+II) response. The stability of the microelectrode has been investigated. The typical potential stability of the studied chalcogenide sensors is within ± 15 mV during two days of intensive measurements in Cd (+II) solutions. Indeed, the nano devices reveal good long-term stability during continuous measurements. This is a favourable feature for measurements in natural water and waste effluents. Moreover, in order to check the reproducibility of experimental out-put signals the potentiometric responses of the sensors were tested more than ten times. The calculated mean values of the slopes of extrapolated straight lines exhibit a standard deviation of ± 3 mV/pCd. The adhesion quality of the thin ISE onto the thin layer collector is satisfying. In fact, a better adhesion between a thin chalcogenide film and the metal will result in a good reproducibility of the sensor behaviour and a longer life time of the sensor.

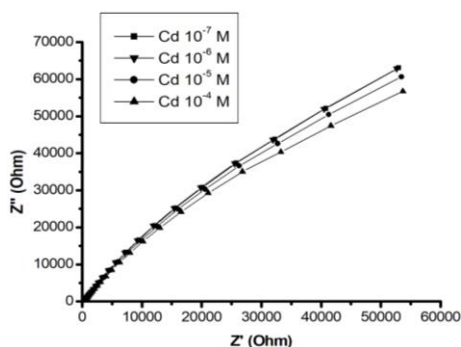


Fig. 5. Complex plane impedance plots of Cd-Ag-Ge₂₈Sb₁₂Se₆₀ in 10^{-1} M KNO_3 electrolyte with different cadmium (+II) concentration.

Impedance spectra for the Cd-Ag-Ge₂₈Sb₁₂Se₆₀ in different solutions of KNO_3 , Cd^{2+} are shown in Fig. 5. The particular shape can be related to the interfacial process at the membrane/solution interface. It could be attributed to a charge transfer, noting that the distinct semicircle shape is less visible and this is typical for a membrane that does not undergo extensive oxidation/corrosion. The impedance spectra revealed the presence of a single time constant due to a charge transfer reaction. Moreover, complex impedance decrease when $[\text{Cd}^{2+}]$ increases indicates that the kinetics of the charge transfer is favoured for an elevated metal concentration. Unfortunately, the expected additional straight line (i. e. silver diffusion) is not observed at lower frequency when the membrane is in contact with concentrated solutions of primary ions [23]. It seems that high complex impedance spectra avoid metal diffusion observation. On the whole, as indicated in MEB investigations, EIS results are in agreement with the low conductivity of the material.

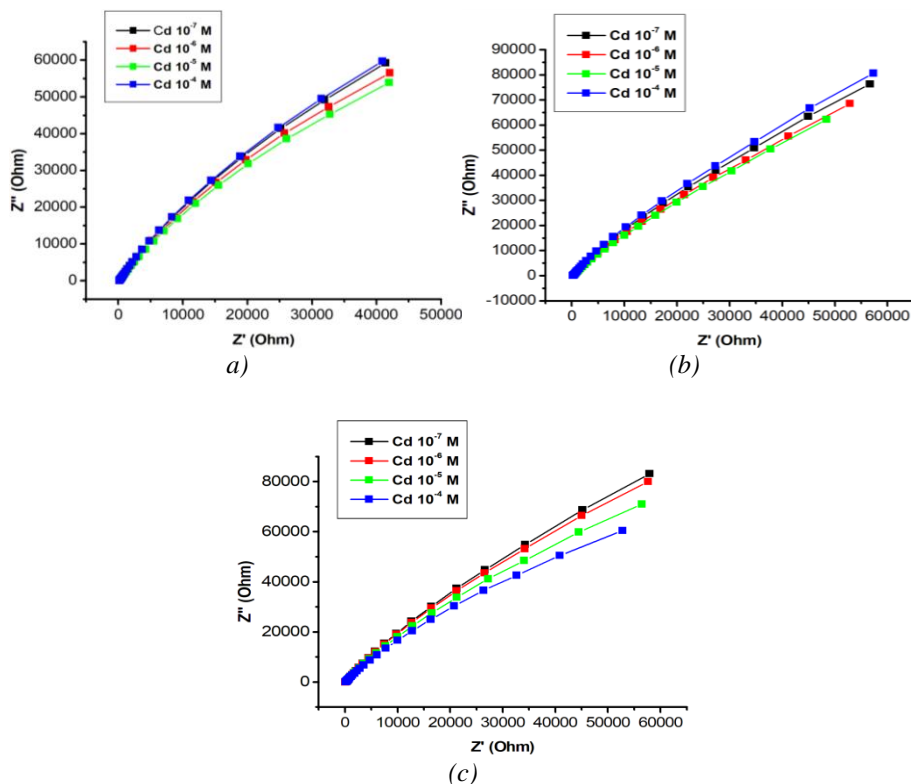


Fig. 6. Complex plane impedance plots of Cd-Ag-Ge₂₈Sb₁₂Se₆₀ in 10^{-1} M KNO₃ electrolyte with different time of aging. 15 min (a), 1 H and half H (b) and 39 H (c).

Ageing study of sensor was done by means of soaking in cadmium (+II) solution. Different impedance spectra of thin film chalcogenide glass are shown in Fig. 6(a), (b), and (c) show the logarithmic representation of the complex impedance plot for different soaking time (i. e. 15 min, 1H30 and 39H) in a Cd²⁺ solution with 10^{-5} M cadmium concentration. Fig. 6 shows that the distinct semicircle nature of the low frequency process gradually disappears and becomes higher (i. e larger diameter) with ageing. The shape of the low frequency semicircle after 1 H 30 of soaking reflects a charge transfer reaction that does not undergo significant thin film oxidation. Moreover, EIS data revealed no changes in the complex impedance as a function of electrode rotation speed. This suggests that the charge transfer reaction is not controlled by diffusion through a fluid boundary layer in the frequency range investigated. As can be seen in Fig. 7, the Bode phase plot shows slight changes in the low frequency range. The increasing phase angle below 1 Hz (Fig. 7 (b)) indicates that the charge transfer reaction becomes less favourable with time. This is commensurate with a slight initial increase in impedance as observed in Fig. 7 (a). The initial increase in phase angle and impedance observed at low frequency implies that the rate of charge transfer between cadmium and the chalcogenide glass becomes hindered, presumably due to the presence of a mild passivation layer. The EIS equivalent circuit helps us to model experimental data. To insure that the equivalent circuit modelling was realistic, it was restricted to a solution resistance in series with one (R, CPE) circuit, which represent the single time constant.

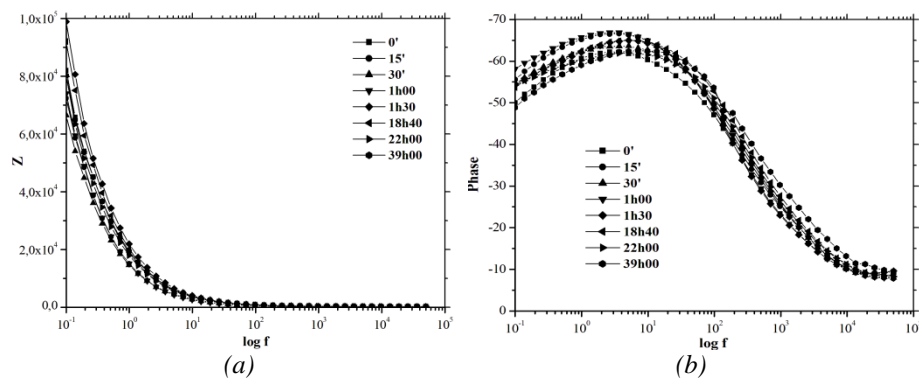


Fig. 7. Bode impedance (a) and Bode phase (b) with different times aging.

4. Conclusions

Micro sensors for the determination of cadmium (+II) species in solution have been developed. Nano materials exhibit satisfying behaviour versus primary ions concentration in laboratory scale. EIS results demonstrated the power of the in-situ technique for elucidating the mechanistic chemistry of the sensing thin film. In agreement with experimental data, we demonstrated that charge transfer process involving two electrons occurs at the membrane – solution interface. Sensitive layer does not undergo extensive oxidation. However, the charge transfer reaction becomes less favourable with aging and this is commensurate with the increase of the impedance.

References

- [1] M. B. Gumpu, S. Sethuraman, U. M. Krishnan, J. B. B. Rayappan. *Sens. Actuators B* **213**, 515 (2015).
- [2] B. Bansod, T. Kumar, R. Thakur, S. Rana, I. Singh. *Biosens. Bioelectron.* **94**, 443 (2017).
- [3] T. V. Moreno, L. C. Malacarne, M. L. Baesso, W. Qu, E. Dy, Z. Xie, J. Fahlman, J. Shen, N. G. C. Astrath. *J. Non-Cryst. Solids* **495**, 8 (2018).
- [4] B. Pejčic, R. De Marco. *Electrochim. Acta* **51**, 6217 (2006).
- [5] F. O. Méar, M. Essi, M.-F. Guimon, A. Pradel, *Chalcogen. Lett.* **5**, 117 (2008).
- [6] W.-J. Song, X.-W. Wang, J.-W. Ding, J. Zhang, R.-M. Zhang, W. Qin. *Chin. J. Anal. Chem.* **40**, 670 (2012).
- [7] E. Baudet, C. Cardinaud, A. Girard, E. Rinnert, K. Michel, B. Bureau, V. Nazabal, *J. Non-Cryst. Solids.* **444**, 64 (2016).
- [8] J. P. Kloock, L. Moreno, A. Bratov, S. Huachupoma, J. Xu, T. Wagner, T. Yoshinobu, Y. Ermolenko, Y. G. Vlasov, M. J. Schöning. *Sens. Actuators B* **118**, 149 (2006).
- [9] M. Essi, D. Cot, *J. Non-Oxide Glasses* **11**, 65 (2019).
- [10] R. Manivannan, S. N. Victoria, *Sol. Energy* **173**, 1144 (2018).
- [11] H. Arida, Q. Mohsen, M. Schöning, *Electrochimica Acta* **54**, 3543 (2009).
- [12] E. Bychkov, M. Bruns, H. Klewe-Nebenius, G. Pfennig, W. Hoffmann, H. J. Ache, *Sens. Actuators B* **24-25**, 733 (1995).
- [13] S. Rondiya, A. Rokade, A. Funde, M. Kartha, H. Pathan, S. Jadkar. *Thin Solids Films* **631**, 41 (2017).
- [14] V. S. Vassilev, S. V. Boycheva. *Talanta* **67**, 20 (2005).
- [15] X. Huang, X. L. Chen, Z. W. Zheng, H. M. Ji, Y. L. Ma, *Chalcogen. Lett.* **16**, 545 (2019).
- [16] P. Sigmund, *Nucl. Instrum. Methods Phys. Res., Sect. B* **27**, 1 (1987)
- [17] Y. Umezawa, P. Bühlmann, K. Umezawa, K. Tohda, S. Amemiya, *Pure Applied Chemistry* **72**, 1851 (2000).
- [18] M. Essi, A. Pradel, *Chalcogen. Lett.* **8**, 301 (2011).

- [19] D. I. Florescu, R. I. Cappelletti, J. Non-Cryst. Solids **246**(1–2), 150 (1999).
- [20] D. Islam, C. E. Brient, R. L. Cappelletti, J. Mater. Res. **5**(3), 511 (1990).
- [21] F. O. Méar, M. Essi, P. Sifat, M.-F. Guimon, D. Gonbeau, A. Pradel, Appl. Surf. Sci. **255**, 6607 (2009).
- [22] C. Cali, G. Taillades, A. Pradel, M. Ribes. Sens. Actuators B **76**, 560 (2001)
- [23] C. Cali, D. Foix, G. Taillades, E. Siebert, D. Gonbeau, A. Pradel, M. Ribes, Mater. Sci. Eng. C **21**, 3 (2002).